Dynamical self-trapping of two-dimensional binary solitons in cross-combined linear and nonlinear optical lattices

K. K. Ismailov ,[1,2] G. A. Sekh ,[3] and Mario Salerno [2]
[1] *Physical-Technical Institute, Uzbek Academy of Sciences, 100084 Tashkent, Uzbekistan*
[2] *Dipartimento di Fisica "E.R. Caianiello", and INFN Gruppo Collegato di Salerno, Universitá di Salerno, Via Giovanni Paolo II, 84084 Fisciano, Salerno, Italy*
[3] *Department of Physics, Kazi Nazrul University, Assansol 713340, India*

(Received 5 May 2023; revised 13 October 2023; accepted 30 October 2023; published 20 November 2023)

Dynamical and self-trapping properties of two-dimensional (2D) binary mixtures of Bose-Einstein condensates in cross-combined lattices, consisting of a one-dimensional (1D) linear optical lattice (LOL) in the x direction for the first component and a 1D nonlinear optical lattice (NOL) in the y direction for the second component, are analytically and numerically investigated. The existence and stability of 2D binary matter wave solitons in these settings are demonstrated both by variational analysis and by direct numerical integration of the coupled Gross-Pitaevskii equations. We find that in the absence of the NOL, binary solitons, stabilized by the action of the 1D LOL and by the attractive intercomponent interaction, can freely move in the y direction. In the presence of the NOL, we find, quite remarkably, the existence of threshold curves in the parameter space separating regions where solitons can move from regions where the solitons become dynamically self-trapped. The mechanism underlying the dynamical self-trapping phenomenon (DSTP) is qualitatively understood in terms of a dynamical barrier induced by the NOL, similar to the Peirls-Nabarro barrier of solitons in discrete lattices. DSTP is numerically demonstrated for binary solitons that are put in motion both by phase imprinting and by the action of external potentials applied in the y direction. In the latter case, we show that the trapping action of the NOL allows one to maintain a 2D binary soliton at rest in a nonequilibrium position of a parabolic trap or to prevent it from falling under the action of gravity. Possible applications of the results are also briefly discussed.

DOI: 10.1103/PhysRevE.108.054218

I. INTRODUCTION

Bose-Einstein condensates (BECs) of ultracold atoms trapped in optical lattices (OLs) are considered as ideal systems for realizing and understanding various phenomena of condensed matter and nonlinear physics. Experimental flexibility of controlling the system parameters over a wide range has made it possible to observe phenomena such as Bloch oscillations, dynamic localization, Landau-Zener tunneling, and superfluid-Mott transition occurring in linear optical lattices (LOLs) [1–9]. In a mean-field description of the condensate, the nonlinearity that arises from the interatomic interactions if suitably balanced by dispersion allows the formation of matter wave solitons [10–12]. This is particularly true for one-dimensional settings where solitons are very stable and quite generic in the whole parameter space.

In higher dimensions and in the presence of attractive interactions, the occurrence of delocalization transitions [13] and the appearance of collapse phenomena induce criticality on the existence of stable solitons [14–16]. The possibility of their stabilization by means of periodic potentials was demonstrated in Refs. [17,18]. In particular, in Ref. [18], it was shown that periodic potentials of codimension 1 (i.e., potentials whose dimension is that of the full space minus one) can support stable solitons both in two-dimensional (2D) and in 3D attractive BECs.

In addition to LOLs, the efficiency in controlling nonlinear interactions in time and space by means of magnetic or optically induced Feshbach resonances has allowed the introduction of the so-called nonlinear optical lattice (NOL), i.e., a lattice induced by space-dependent interatomic interactions. The effective potential produced by a NOL can be periodic or localized, depending on whether the density of matter is periodic or localized.

In one-dimensional settings, NOLs have been shown to be very useful to eliminate destructive dynamical instabilities, such as those arising in Bloch oscillations of gap solitons moving in an accelerated LOL [19]. In the multidimensional case, it is proven that 2D localized BEC can be stable in 1D cross-combined linear and nonlinear optical lattices [20], but neither a 1D NOL nor a 2D NOL are sufficient to hold stable 2D BECs [21]. In nonlinear optics contexts, it was recently shown that NOLs of the form of arrays of Kerr-nonlinear cylinders embedded into linear [22] or saturable host media can support stable 2D solitons [23]. We also remark that the existence of 2D Bose-Einstein condensates has been realized experimentally in a combination of harmonic and lattice potentials [24–26] and all the studies reported above refer to the case of ordinary, i.e., single-component, BECs.

Multidimensional solitons of binary BEC mixtures are more involved and much less investigated [27]. In particular, we mention the results in Ref. [28] showing that either a 2D LOL or a 2D NOL applied only to one component is sufficient to stabilize binary 2D BEC solitons against collapse or decay. In the case of a LOL, the binary solitons were shown to be stable on almost the entire range of their existence, while in the NOL case, there were restrictions on the number of atoms in the component affected by the lattice. In all these cases, the applied OLs (either linear or nonlinear) were two dimensional and the resulting excitation was intrinsically localized.

On the other hand, it is interesting to investigate 2D solitons of binary BEC mixtures trapped in lower-dimensional OLs of a different nature. In this respect, we remark that in contrast with 1D LOLs, a 1D NOL is unable to sustain stable 2D solitons and therefore, in a cross-combined setting (i.e., a 1D LOL and a 1D NOL acting in different directions), binary solitons can exist only if the attractive intercomponent interaction is sufficiently strong. Moreover, the different nature of the two lattices could lead to novel dynamical phenomena.

The aim of the paper is to investigate the properties of 2D solitons of binary BEC mixtures trapped in cross-combined OLs consisting of a 1D LOL acting on one component along the x direction and a 1D NOL acting on the other component along the y direction. For this, we use the variational analysis (VA), direct numerical integrations of the coupled Gross-Pitaevskii equations (GPE), and the Vakhitov-Kolokolov (VK) criterion [29] to investigate the existence and the stability of 2D binary solitons in such cross-combined OLs. We show that in the absence of the NOL, binary 2D solitons, stabilized by the action of the 1D LOL and by the attractive intercomponent interaction, can be put into action by phase imprinting and move freely in the y direction. In the presence of the NOL, quite remarkably, we find the existence of threshold curves in the parameter space separating regions where solitons can move from regions where they becomes dynamically self-trapped by the NOL.

The mechanism underlying the dynamical self-trapping phenomenon (DSTP) is qualitatively explained in terms of a dynamical barrier induced by the the NOL that resembles the Peirls-Nabarro barrier [30] of solitons in discrete lattices. The DSTP is demonstrated for binary solitons that are put in motion both by phase imprinting and by the action of external potentials applied in the y direction, such as a parabolic trap or a linear ramp potential. In these cases, we show that the DSTP allows one to hold a 2D binary soliton at rest in a nonequilibrium position of a parabolic trap and to prevent the soliton from falling under the action of the gravity.

The paper is organized as follows. In Sec. II, we introduce the model equations, and in Sec. III, we use the variational analysis and numerical GPE integrations to investigate the existence and stability of 2D binary isotropic and anisotropic solitons. In Sec. IV, we use the phase-imprinting method to put stationary solitons in motion and to show the occurrence of the DSTP. In Sec. V, the occurrence of the DSTP in external parabolic traps and linear ramp potentials is demonstrated. In Sec. VI, the possible relevance of the DSTP for application is briefly discussed and the main results are summarized.

II. MODEL EQUATIONS

At absolute zero temperature, the ground-state wave functions of a 2D binary BEC mixture can be described in the mean-field approximation by the following coupled Gross-Pitaevskii (GP) equations:

$$i\frac{\partial\psi}{\partial t} = -(\nabla^2 - V_L - \gamma_1|\psi|^2 - \gamma_{12}|\phi|^2)\psi, \tag{1}$$

$$i\frac{\partial\phi}{\partial t} = -(\nabla^2 - V_{NL}|\phi|^2 - \gamma_2|\phi|^2 - \gamma_{12}|\psi|^2)\phi, \tag{2}$$

where ∇^2 denotes the 2D Laplacian and V_L, V_{NL} are periodic real functions modeling a LOL in the x direction and a NOL in the y direction, respectively, of the form

$$V_L = V_1\cos(2x), \quad V_{NL} = V_2\cos(2y). \tag{3}$$

In Eqs. (1) and (2), ψ and ϕ represent the component wave functions, while the nonlinear coefficients γ_i, $i = 1, 2, 12$ stand for 3D coupling constants corresponding to the s-wave scattering lengths $a_s^{(i)}$, i.e., $\gamma_i = 4\pi\hbar^2 a_s^{(i)}/m$, with m, $l_z = \sqrt{\hbar/(m\omega_z)}$, ω_z, denoting the atom mass, the transverse oscillator length, and the transverse frequency, respectively. The above GPEs are written in dimensionless units obtained by replacing t by $(\hbar/E_r)t$, and $r \equiv (x, y)$ by r/k, with $E_r = \hbar^2k^2/(2m)$ the recoil energy of the lattices, and V_j, γ_j measured in the units of E_r and E_r/k^2, respectively.

It is also worthwhile to note from Eqs. (1) and (2) that while the first component is trapped by the potential V_L acting in the x direction, the second component is subjected to a nonlinear optical lattice V_{NL} acting in the y direction. For this, we assume the BEC components are associated to two hyperfine levels that are far detuned so that the laser used for the trapping of one component can be considered negligible for the other component, and vice versa. The spatial modulation of the interatomic scattering length can be produced by the optically induced Feshbach resonance technique, with the background scattering length assumed to be detuned to zero with appropriate experimental conditions. Moreover, the harmonic trap used to create the condensate is assumed to be weak enough to affect matter waves localized in the central part of the trap [9].

III. 2D BINARY SOLITONS: VA AND NUMERICAL RESULTS

In this section, we investigate the existence and stability properties of 2D binary solitons by means of the VA [31] based on the Gross-Pitaevskii energy density,

$$E[\psi,\phi] = |\nabla\psi|^2 + |\nabla\phi|^2 + V_1\cos(2x)|\psi|^2 + \tfrac{1}{2}\gamma_1|\psi|^4 + \tfrac{1}{2}V_2\cos(2y)|\phi|^4 + \tfrac{1}{2}\gamma_2|\phi|^4 + \gamma_{12}|\phi|^2|\psi|^2. \tag{4}$$

Results are then compared with direct numerical integration of the GPE system. With respect to perturbation theory, the VA represents a simple effective method to get properties of the ground-state wave function. The efficiency and accuracy of the method depend in large part on the choice of the trial function that should reflect, from one side, the properties of the system (symmetries, norms, etc.), and, from the other side, should be simple enough to allow an analytical evaluation of the energy. The trapping potentials, the type of solutions that are searched (localized, extended), and the parameter region in which they are searched also play an important role for the choice. Thus, for example, looking for localized binary matter waves in the limit of negligible trapping potentials, one could take the trial function as a product of 1D solitons (sech-sech trial functions), while in the limit of negligible nonlinearities, the Gaussian ansatz may be more appropriate. We tried both *Ansätze* for our setting and we found that the Gaussian *Ansatz* allows an analytical expression of the energy for generic values of the parameters (see below), while with the sech-sech *Ansatz*, this is possible only when the NOL is absent [32]. In the following, therefore, we assume a Gaussian *Ansatz* for the component wave functions,

$$\psi(x,y) = A_1 \exp\left[-x^2/\left(2a_1^2\right) - y^2/\left(2b_1^2\right)\right], \tag{5}$$

$$\phi(x,y) = A_2 \exp\left[-x^2/\left(2a_2^2\right) - y^2/\left(2b_2^2\right)\right], \tag{6}$$

with corresponding norms given by

$$\mathcal{N}_1 = \int |\psi|^2 dxdy = \pi a_1 b_1 A_1^2,$$
$$\mathcal{N}_2 = \int |\phi|^2 dxdy = \pi a_2 b_2 A_2^2. \tag{7}$$

Here, a_j, b_j, $j = 1, 2$, denote the widths of the two component profiles in the x and y directions, respectively, and A_j the corresponding profile amplitudes. Similar trial solutions were used in Refs. [17,18,20,21] to describe solitons ($a_j/\pi \leqslant 1$) in single-component two-dimensional BECs in OLs. The integration of the energy density (4) on the whole $x-y$ plane leads to the following effective energy:

$$\langle E\rangle = \sum_{j=1}^{2}\left[\frac{\mathcal{N}_j}{2}\left(\frac{1}{a_j^2}+\frac{1}{b_j^2}\right)+\frac{\gamma_j\mathcal{N}_j^2}{4\pi a_j b_j}\right] + V_1\mathcal{N}_1 e^{-a_1^2} + \frac{V_2\mathcal{N}_2^2}{4\pi a_2 b_2}e^{-\frac{b_2^2}{2}} + \frac{\gamma_{12}\mathcal{N}_1\mathcal{N}_2}{\pi\left[\left(a_1^2+a_2^2\right)\left(b_1^2+b_2^2\right)\right]^{\frac{1}{2}}}. \tag{8}$$

Notice that in writing this equation, we used Eqs. (7) to eliminate A_j in favor of $[\mathcal{N}_j/(\pi a_j b_j)]^{\frac{1}{2}}$. The stationary conditions $\frac{\partial\langle E\rangle}{\partial a_i} = 0$, $\frac{\partial\langle E\rangle}{\partial b_i} = 0$, $i = 1, 2$, of the energy function in Eq. (8) provide a system of four equations, namely,

$$\frac{1}{a_1^3} + \frac{\gamma_1\mathcal{N}_1}{4\pi a_1^2 b_1} + \frac{a_1}{\pi}\gamma_{12}\mathcal{N}_2 F_1 + 2V_1 a_1 e^{-a_1^2} = 0, \tag{9}$$

$$\frac{1}{b_1^3} + \frac{\gamma_1\mathcal{N}_1}{4a_1 {b_1}^2\pi} + \frac{b_1}{\pi}\gamma_{12}\mathcal{N}_2 F_2 = 0, \tag{10}$$

$$\frac{1}{a_2^3} + \frac{a_2}{\pi}\gamma_{12}\mathcal{N}_1 F_1 + \mathcal{N}_2\frac{\gamma_2 + e^{-\frac{b_2^2}{2}}V_2}{4\pi a_2^2 b_2} = 0, \tag{11}$$

$$\frac{1}{b_2^3} + \mathcal{N}_2\frac{\gamma_2 + \left(1+{b_2}^2\right)e^{-\frac{{b_2}^2}{2}}V_2}{4\pi a_2 {b_2}^2} + \frac{b_2}{\pi}\gamma_{12}\mathcal{N}_1 F_2 = 0, \tag{12}$$

with $F_1 = (a_1^2+a_2^2)^{-3/2}(b_1^2+b_2^2)^{-1/2}$ and F_2 obtained from F_1 by interchanging the b's with a's. To obtain parameters for the existence of binary BEC solitons, in general, one must solve Eqs. (9)–(12) numerically. For some specific choice of the system parameters, the energy of the system displays a minimum that is, in general, negative. Binary solitons follow from Eqs. (5) and (6) with parameters A_i, a_i, b_i, $i = 1, 2$, determined in correspondence with the energy minimum.

The stability of the soliton can be analytically investigated within a VA approach by means of the VK criterion [29,33] according to which a binary soliton is stable if the change of a corresponding conserved (numbers of atoms, $\mathcal{N}_j$) quantity with respect to its conjugated variable (chemical potential μ_j) is negative.

In this respect, it is worthwhile to note that for stationary solutions,

$$\phi \equiv \phi(x,y)\exp(-i\mu_1 t), \quad \psi \equiv \psi(x,y)\exp(-i\mu_2 t),$$

the GPEs in (1) and (2) can be rewritten as

$$\mu_1 = \frac{1}{\mathcal{N}_1}\int (|\nabla\psi|^2 + V_L|\psi|^2 + \gamma_1|\psi|^4 + \gamma_{12}|\phi|^2|\psi|^2)d\tau, \tag{13}$$

$$\mu_2 = \frac{1}{\mathcal{N}_2}\int (|\nabla\phi|^2 + V_{NL}|\phi|^4 + \gamma_2|\phi|^4 + \gamma_{12}|\psi|^2|\phi|^2)d\tau, \tag{14}$$

with $d\tau = dxdy$. Substituting Eqs. (3), (5), and (6) into Eqs. (13) and (14), we get

$$\mu_1 = \frac{1}{2}\left(\frac{1}{a_1^2}+\frac{1}{b_1^2}\right) + \frac{\gamma_1\mathcal{N}_1}{2\pi a_1 b_1} + V_1 e^{-a_1^2} + \frac{\gamma_{12}\mathcal{N}_2}{\pi\sqrt{\left(a_1^2+a_2^2\right)\left(b_1^2+b_2^2\right)}} \tag{15}$$

and

$$\mu_2 = \frac{1}{2}\left(\frac{1}{a_2^2}+\frac{1}{b_2^2}\right) + \frac{V_2\mathcal{N}_2}{2\pi a_2 b_2}e^{-b_2^2/2} + \frac{\gamma_{12}\mathcal{N}_1}{\pi\sqrt{\left(a_1^2+a_2^2\right)\left(b_1^2+b_2^2\right)}} + \frac{\gamma_2\mathcal{N}_2}{2\pi a_2 b_2}. \tag{16}$$

From the above equations, one can calculate the derivatives $d\mathcal{N}_j/d\mu_j$ and then, from the VK criterion, determine the stability of the soliton. This is shown in Fig. 2 for a specific choice of the parameters (see below).

In the following two sections, we consider in more detail the cases of isotropic and anisotropic 2D binary solitons and compare the VA analytical predictions with numerical direct GPE time integrations.

A. Isotropic 2D binary solitons

To understand the behavior of the BEC profile embedded in a LOL and NOL, we first consider the symmetric case $b_i = a_i$, $i = 1, 2$, but with $a_1 \neq a_2$, giving rise to isotropic component profiles in the x and y directions. For simplicity, in the following, we fix $\gamma_2 = 0$, i.e., we assume the intraspecies scattering length of the second component detuned to zero by a Feshbach resonance.

One can then show that the minimization of the effective energy, $\langle\tilde{E}\rangle \equiv \langle E\rangle|_{b_i\to a_i}$, with respect to the a_1 variable, i.e., $\frac{\partial\langle\tilde{E}\rangle}{\partial a_1} = 0$, gives

$$a_2 = \left[\sqrt{\frac{-\gamma_{12}\mathcal{N}_2}{\pi\left(1+a_1^4 V_1 e^{a_1^2}\right)+\gamma_1\mathcal{N}_1/4}} - 1\right]^{\frac{1}{2}} a_1, \tag{17}$$

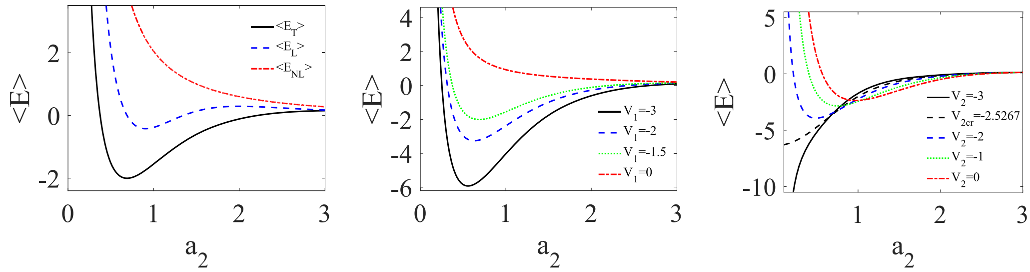

FIG. 1. Left panel: Effective energy potential $\langle E\rangle$ vs a_2 for uncoupled symmetric ($a_i = b_i$) components (blue dashed and red dash-dotted curves), and for the coupled $\gamma_{12} = -2$ case (solid black curve). Other parameters are fixed as $\gamma_1 = -2$, $\gamma_2 = 0$, $V_1 = -1.5$, $V_2 = -1.5$, $\mathcal{N}_1 = 3.5$, and $\mathcal{N}_2 = 2.5$. Middle panel: Same as in the left panel, but for $\gamma_{12} = -2$, $V_2 = -1.5$ and different values of V_1 indicated in the figure. Other parameters are fixed as in the left panel. Values of a_1 and a_2 are calculated at the minima of the depicted bonding curves. Right panel: Same as in the middle panel, but for $V_1 = -2$ and different values of V_2 indicated in the figure. Other parameters are fixed as in the middle panel.

while the minimization with respect to a_2, i.e., $\frac{\partial\langle\tilde{E}\rangle}{\partial a_2} = 0$, allows one to express a_1 in terms of a_2 as

$$a_1 = \left[\sqrt{\frac{-\gamma_{12}\mathcal{N}_1}{\pi + \left(1 + a_2^2/2\right)e^{-a_2^2/2}V_2\mathcal{N}_2/4}} - 1\right]^{\frac{1}{2}} a_2. \tag{18}$$

Note that both Eqs. (17) and (18) allow energy to be expressed in terms of a single variable. Due to the different nature of linear and nonlinear OLs, however, the two minimizations cannot be performed together and one must choose one or the other. In fact, it can be shown that the compatibility condition of (18) and (17) is, in general, not satisfied for generic values of the parameters [34]. Since a_2 is the variable of the component exposed to the action of the NOL, whose stability is more critical, it is natural to choose to minimize with respect to a_2, i.e., Eq. (18). This choice is corroborated by the fact that by inserting the expression of a_1 into the energy and plotting it as a function of a_2, one obtains bounding potential curves (see Fig. 1), while the other option would lead to metastable or antibounding curves.

In the limit $\gamma_{12} \to 0$, Eqs. (1) and (2) become uncoupled and the problem further simplifies to two independent (single-component) BECs, i.e., one loaded in a LOL and the other in a NOL, with the corresponding energy vs a_2 curves denoted as $\langle E_L\rangle$ and $\langle E_{NL}\rangle$, respectively. In the left panel of Fig. 1, we show the dependence of these energies on the parameter a_2, both for the coupled and uncoupled cases. Notice the resemblance of these curves with the energy-potential curves of a diatomic molecule, with a_2 playing the role of interatomic distance. From these curves, it is clear that while the single-component 2D BEC in the 1D LOL is energetically stable, i.e., the BEC mixture is in a bonding state (blue dashed curve), as expected from the results in Ref. [24], no 2D soliton can be formed in a single-component BEC with a NOL since the system is in an antibonding state (red dash-dotted curve) when $\gamma_{12} = 0$. When $\gamma_{12} \neq 0$, however, the energy-potential curve develops a deeper minimum (with respect to $\langle E_L\rangle$) that allows both components to hold together in a bound state (black solid curve). This makes the components of the 2D solitons intrinsically interdependent since the presence of the inter-component attraction and the stability of the first component are essential for the localization of the second component and for the bound state formation. In the middle and right panels of Fig. 1, we show the dependence of the $\langle E\rangle$ vs a_2 curves for different values of V_1, keeping V_2 fixed, and vice versa, respectively.

In particular, from the middle panel of Fig. 1, it is clear that for $V_1 = 0$ (absence of the LOL), there is no possibility to form any stable bound state, but as V_1 is decreased away from zero, the potential develops a local minimum that becomes deeper and deeper as V_1 is further decreased. This indicates that for fixed parameters and sufficiently strong LOL, symmetric binary BEC solitons can exist in the cross-combined OLs system. The minima of the effective energy ($\langle E\rangle_{\min}$) for the $V_1 = -1.5, -2, -3$ occur at $a_2 \approx 0.69, 0.63$, and 0.55, respectively. Clearly, $\langle E\rangle_{\min}$ is positive for $V_1 = 0$. It indicates that the system becomes unstable for a weak LOL.

From the right panel of Fig. 1, it is also clear that by increasing the strength, V_2, of the NOL, and keeping all other parameters fixed, the local minimum of the effective potential disappears at a critical value V_{2cr} (for the specific choice of parameters, $V_{2cr} \approx -2.53$). We find that the minimum of $\langle E\rangle$ occurs for $V_2 = 0, -1, -2$ at $a_2 \approx 0.97$, 0.75, 0.49, respectively. The thin black curve gives the lower boundary of the potential curve below which the system is collapsed ($a_1 = a_2 = 0$ for $V_1 = -2.0$ and $V_2 = -2.52$).

We have seen that the interplay between the LOL and NOL acting in two different directions plays a role in holding 2D BEC solitons stable. The effective energy of the system shows minima and can diverge depending on the relative values of the LOL and NOL. This indicates some possibilities for the observation of stable, unstable, and collapse phenomena. It is, therefore, constructive to check the profiles of the binary condensates from the direct numerical simulation of the GPEs. In particular, in the following, we use the split-step Fourier (SSF) method [21] to study the spatiotemporal behavior of BECs. The SSF is a pseudospectral method and very efficient in solving a nonlinear partial differential equation [35–37] with a very small time step. With a view to calculate the evolution of the condensate in 2D, we consider a time step $\Delta t = 0.001$ and calculate the density of the BEC components. In each step, we propagate the solution by half a time step ($\Delta t/2$) using a nonlinear operator and then a full time step (Δt) with a linear operator; then the propagation is completed by the second half

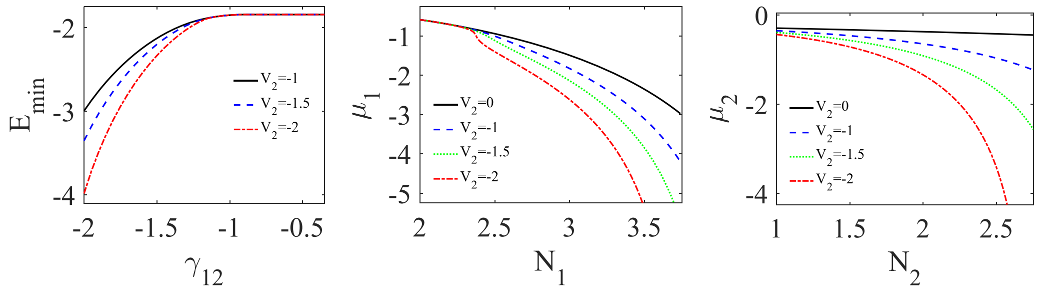

FIG. 2. Left panel: Minimum energy ($E_{\min}$) as a function of γ_{12} for $V_2 = -1$ (solid black), -1.5 (dashed blue), and -2 (dash-dotted red). Other parameters of the system are fixed as $\gamma_1 = -2$, $V_1 = -2$, $\mathcal{N}_1 = 3.5$, and $\mathcal{N}_2 = 2.5$. Middle and right panels: Chemical potentials μ_i vs number of atoms, N_i, of first (middle) and second (right) component, for strengths (V_2) of the NOL indicated in the figure. Other parameters are fixed as $\gamma_1 = -2$, $\gamma_{12} = -2.0$, $V_1 = -2.0$.

step (Δt) with a nonlinear operation. More explicitly,

$$\psi(x, y, t + \Delta t) = e^{-iL_\psi \Delta t/2} \mathcal{F}^{-1}\left[e^{-i(k_x^2+k_y^2)\Delta t} \mathcal{F} \times \{e^{-iL_\psi \Delta t/2}\psi(x, y, t)\}\right] \tag{19}$$

and

$$\phi(x, y, t + \Delta t) = e^{-iL_\phi \Delta t/2} \mathcal{F}^{-1}\left[e^{-i(k_x^2+k_y^2)\Delta t} \mathcal{F} \times \{e^{-iL_\phi \Delta t/2}\phi(x, y, t)\}\right], \tag{20}$$

with $L_\psi = V_1 \cos(2x) + \gamma_1|\psi|^2 + \gamma_{12}|\phi|^2$ and $L_\phi = V_2 \cos(2y)|\phi|^2 + \gamma_2|\phi|^2 + \gamma_{12}|\psi|^2$. Here, $\mathcal{F}$ and $\mathcal{F}^{-1}$ stand for Fourier and inverse Fourier transforms, respectively.

Clearly, Eqs. (19) and (20) give the time evolution of the condensate profiles for the first and second components, respectively. In particular, the dynamical stability of the stationary solution is obtained from time evolution of the initial states [38]. In Figs. 3 and 4, we plot the component densities of the 2D binary BEC at time $t = 100$, as obtained from numerical GPE time integration in the absence and in the presence of the NOL, respectively. We see that in both cases, the density profiles remain stable without changing their norms on a long timescale. Also notice that the VA profiles (see blue lines) are in reasonably good agreement with the ones obtained numerically by imaginary time evolution.

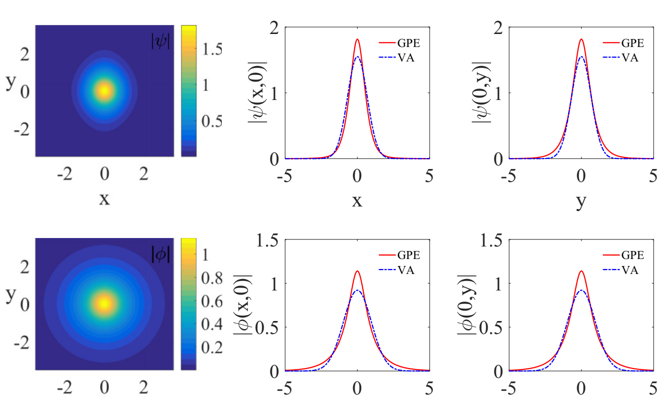

FIG. 3. 2D density plot at time $t = 100$ (left) and corresponding 1D sections at $y = 0$ (middle) and at $x = 0$ (right) of the first (top panels) and second (bottom panels) components of the 2D BEC soliton. Parameters values are fixed as $V_1 = -2.0$, $V_2 = 0$, $\gamma_1 = -2.0$, $\gamma_2 = 0$, $\gamma_{12} = -2.0$, $\mathcal{N}_1 = 3.5$, $\mathcal{N}_2 = 2.5$. The initial numerical profiles (red lines) overlap the ones at time $t = 100$. Blue lines refer to the initial profiles predicted by the VA, plotted for comparison.

B. Anisotropic 2D binary solitons

We have seen that the consideration of an isotropic condensate can provide a simplified system and allow us to realize the system's properties in terms of the potential model. However, a more general study needs to remove the restriction on the condensate size in different directions. Therefore, it will also be constructive to consider $b_i \neq a_i$, ($i = 1, 2$) and $a_1 \neq a_2$.

In order to see the effect of intercomponent interaction to the energy of the system, we solve Eqs. (9)–(12) numerically and calculate the minimum energy ($E_{\min}$) for different values of intercomponent interaction. The variation of $E_{\min}$ with γ_{12} is displayed in the left panel of Fig. 2. It is seen that the minimum energy is negative for some nonzero values of interspecies interaction. This clearly indicates the existence of stable BECs. Looking closely at the figure, we see that $E_{\min}$ depends sensitively on the interplay between optical lattices and interspecies interaction. More specifically, $E_{\min}$ decreases rapidly for larger values of $-\gamma_{12}$. This change in $E_{\min}$, however, becomes less noticeable at smaller values of γ_{12}.

The slopes of the μ_j versus $\mathcal{N}_j$ displayed in the middle and right panels of Fig. 2 show that $d\mu_j/d\mathcal{N}_j$ is negative and thus consistent with the VK criterion for linear stability.

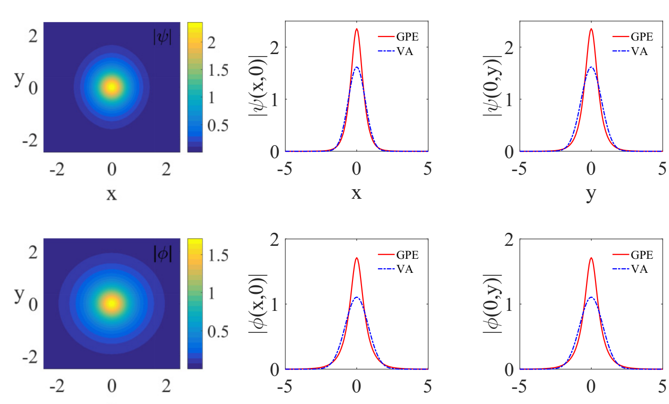

FIG. 4. Same as in Fig. 3, but for $V_2 = -1$.

With a view to study the dynamical stability, we calculate the density profile by numerically solving Eqs. (1) and (2) at three different times using Eqs. (19) and (20). We take the linearly stable stationary solution as the initial profile and display the final profiles in Fig. 4. It is clear from the time evolution that the coupled BECs in 2D are dynamically stable due to the interplay between nonlinearity (steepening) and dispersive effects.

Note that in the presence of the NOL, the agreement between the VA soliton profiles and the ones from GPE numerical calculations becomes less accurate and more qualitative. This is probably due to the fact that the Gaussian trial functions do not allow one to catch the full symmetry of the cross-combined lattice. The VA stability predictions obtained with the VK criterion, however, were always confirmed by the numerical GPE integrations, at least for the parameters values that we have investigated.

We finally remark that as expected for multidimensional settings with attractive interactions, the above 2D binary solitons can undergo the collapse phenomenon. Indeed, we find that the stability depends on the norms, strength of the attractive interactions, and strength of the OLs, and for each of these parameters there exist critical values above which the collapse occurs. The study of the collapse phenomenon in our setting, however, requires more detailed analytical and numerical investigations that are beyond the aim of this paper.

IV. SELF-TRAPPING ACTION OF THE NOL

To understand the trapping action exerted by the NOL on a binary 2D BEC soliton, it is convenient to first consider the case in which there is only the LOL in the x direction. In this case, a binary 2D matter wave, stabilized by the action of the 1D LOL and by the attractive intercomponent interaction, can freely move in the y direction. This is shown in the top panels of Fig. 5 where an initial velocity v_0 in the y direction has been given to the stationary components ψ, ϕ (obtained from imaginary-time evolution) by means of the phase imprinting,

$$\psi \to \psi e^{iv_0(y-y_0)}, \quad \phi \to \phi e^{iv_0(y-y_0)}.$$

This state is then used as the initial condition for the real-time integration of the coupled GPE system. The results are reported in Fig. 5 for a fixed imprinted velocity and different values of the strength of the NOL. We see that in the absence of the NOL, the 2D binary matter wave moves like a soliton, retaining its shape and initial velocity, while in the presence of the NOL and for a fixed imprinted velocity, the soliton can either move or become dynamically self-trapped (i.e., oscillates around some positions), depending on the strength of the NOL being below or above a certain threshold, respectively. Notice that the amplitude of the period of the oscillations in the self-trapped regime decreases by increasing the strength of the NOL, with the binary soliton becoming fully at rest for sufficiently high values of V_2 (in Fig. 5, this occurs for $V_2 = -2.0$, as one can see from the bottom panel).

The origin of the self-trapping can be qualitatively understood by taking into account the effective potential, $\mathcal{V}_{\rm NOL}$, induced by the NOL on the moving second component. For simplicity, we assume for this a solitary wave localized in a minimum of the LOL (i.e., stationary with respect to the LOL)

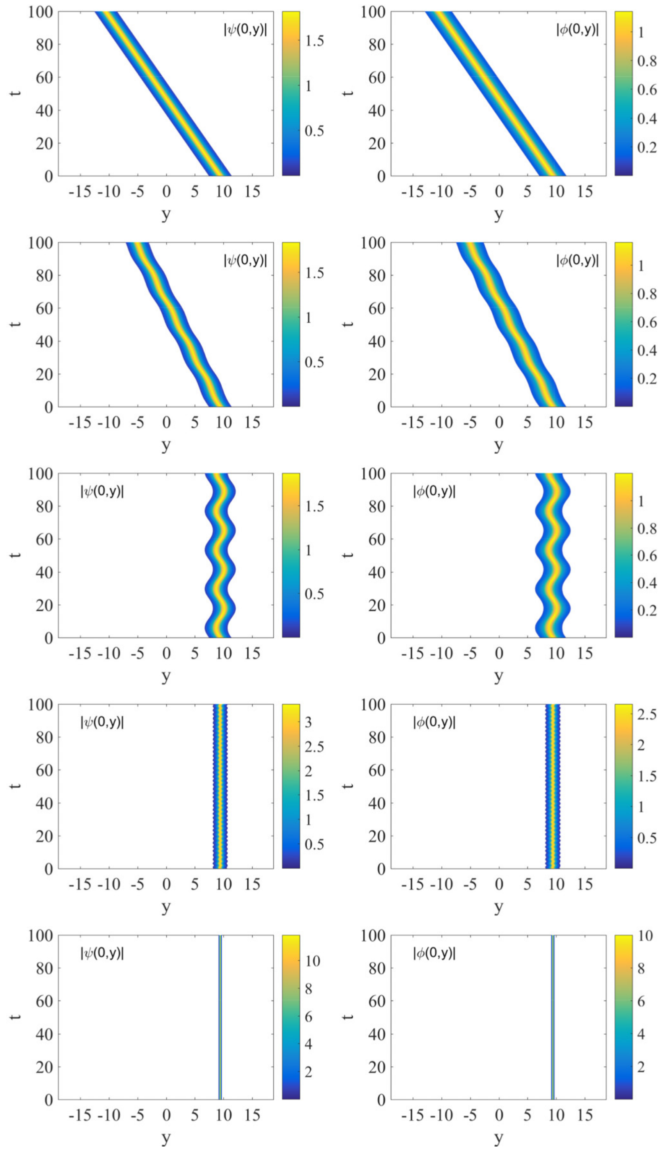

FIG. 5. Density plots of the dynamics of a 2D binary soliton with phase-imprinted velocity along the y direction. Panels, from top to bottom, refer to the different strengths of the NOL, i.e., $V_2 = 0.0, -0.05, -0.15, -1.5, -2.0$, respectively, while left and right panels refer to the first and second component, respectively. The velocity v_0 is imprinted by multiplying the stationary BEC components by the phase factor $\exp[-iv_0(y-y_0)]$ with $v_0 = 0.1$ and $y_0 = 3\pi$. Other parameters are fixed as $V_1 = -2.0$, $\gamma_1 = -2.0$, $\gamma_2 = 0.0$, $\gamma_{12} = -2.0$, $N_1 = 3.5$, $N_2 = 2.5$.

moving with constant velocity v_0 in the y direction. In this case, the effective NOL potential has the form

$$\mathcal{V}_{\rm NOL} = V_2 \cos(2y)|\phi(x, \zeta(t))|^2, \tag{21}$$

with $\zeta(t) = y - v_0 t$ denoting the traveling wave coordinate. Notice that the potential in Eq. (21) is periodic in y (with period equal to π) and that while the density profile depends on time, the sinusoidal factor is independent of t, being related to the stationary wave that spatially modulates the intraspecies interaction of the second component via an optically induced Feshbach resonance.

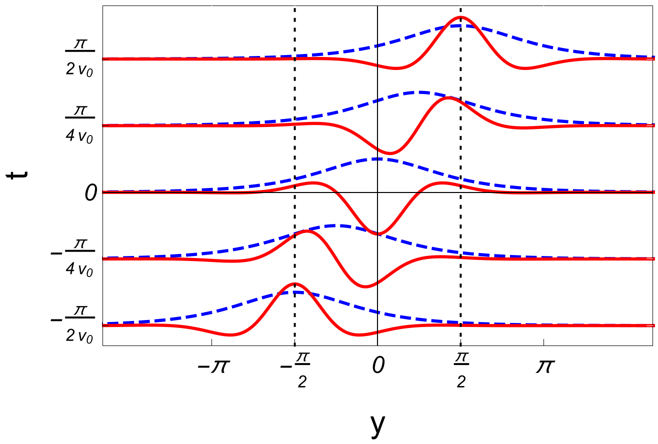

FIG. 6. Schematic representation of the NOL effective potential in Eq. (21) (continuous red lines) and of the density profiles (dashed blue lines) as functions of y and at t. For simplicity, we assumed, for the density y section, a solitary wave profile of the form $\frac{1}{\sqrt{2}}\mathrm{sech}(y - v_0 t)$ and fixed parameters as $v_0 = 0.5, V_2 = -2.5$. Vertical dotted lines show the edges of the periodicity y interval.

As the BEC density moves, the shape of the potential changes in the periodicity interval $y \in [-\pi/2, \pi/2]$, as schematically shown in Fig. 6. We see that at $t = 0$ ($y = 0$), the soliton density is located at the minimum of $\mathcal{V}_{\rm NOL}$ (which has the form of a potential well) and at $t = \pm\pi/2v_0$ (i.e., $y = \pm\pi/2$) it is located at the maximum of $\mathcal{V}_{\rm NOL}$ (which has the form of a potential barrier). In order to move then, the soliton must have at least the energy necessary to overcome the potential barriers faced at the edges of the periodicity interval of $\mathcal{V}_{\rm NOL}$. On the contrary, the localized matter wave remains trapped inside the NOL effective potential and oscillates around its minimum. This bears resemblance to the Peirls-Nabarro barrier that discrete solitons must overcome in order to move [30]. In our case, however, the barrier depends on the dynamics and is self-created by the wave through its density; for this, we refer to it as *dynamical self-trapping* barrier.

As is well known, the effect of the usual Peirls-Nabarro barrier on discrete solitons is the slowing down of their motion and eventually their stopping (pinning) at some lattice site. These behaviors are similar to what we observe in our numerical experiments (see below). In the presence of attractive intercomponent interaction, necessary for the binary 2D soliton to exist, the stopping of the second component implies the stopping of the first component as well, and therefore the dynamical self-trapping of the 2D binary soliton. This qualitatively explains the physical mechanism by which the DSTP arises in the presence of the NOL [39].

V. DSTP IN EXTERNAL POTENTIALS

Dynamical behaviors similar to the ones of the previous section are expected for binary BEC solitons put in action by external potentials. In the absence of the NOL (i.e., with only the LOL in the x direction), we find (see below) that the addition of a parabolic trap in the y direction makes the soliton oscillating around the minimum of the potential, while the addition of a ramp potential produces a uniform acceleration along the y direction, just as one would expect for ordinary solitons.

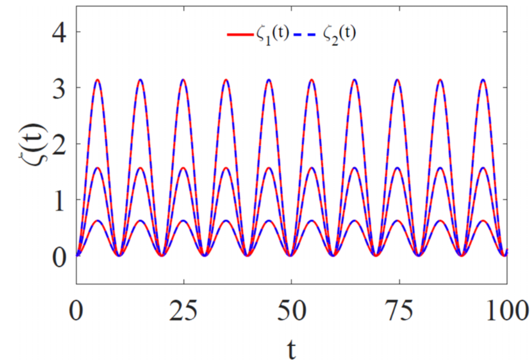

FIG. 7. The dynamics of the COM coordinates of a binary soliton in a parabolic trap $\beta(y - y_0)^2$, in the absence of the NOL ($V_2 = 0$) for different initial trap displacements, i.e., $y_0 = 0.1\pi, 0.25\pi, 0.5\pi$, corresponding to curves with amplitudes ordered from smaller to larger, respectively. Other parameters are fixed as $\beta = 0.1$, $\gamma_1 = -2.0$, $\gamma_2 = 0$, $\gamma_{12} = -2.0$, $V_1 = -2.0$, $N_1 = 3.5$, $N_2 = 2.5$. Note that the COM curves of the two components are perfectly overlapping.

The presence of the NOL in the y direction, however, introduces the possibility of dynamical self-trapping phenomena intuitively expected when the soliton energy is not enough for the overcoming of the effective NOL barrier discussed before. This automatically implies the existence of thresholds in the parameter space, as demonstrated in the following sections for the specific cases of parabolic traps and linear ramp potentials.

To show this, we recourse to numerical integration of the coupled GPE system taking binary solitons obtained from imaginary-time evolution as initial conditions. The potentials are applied in all cases along the y direction and the center of mass of the initial conditions are located at the ($x = 0, y = 0$) position in the cross-combined potential. With this setup, the motion of the binary soliton along the x axis is strongly confined by the LOL to the $x = 0$ channel and the dynamics mainly occurs in the y direction (this is particularly true for a deep LOL and strong intercomponent interactions). The dynamics is then investigated in terms of the center of mass (COM) of the two BEC components defined by

$$\zeta_j(t) = \frac{\iint_{-\infty}^{\infty} y\,|\psi_j|^2 dxdy}{\iint_{-\infty}^{\infty} |\psi_j|^2 dxdy}, \quad j = 1, 2. \tag{22}$$

A. Parabolic trap

A parabolic trap of the form $\beta(y - y_0)^2$, with β and y_0 real parameters controlling the strength and the position of the trap minimum, respectively, is applied to both components of the binary matter wave. The initial condition is taken as a stationary binary soliton at the position $x = 0$, $y = 0$ obtained from imaginary time with the trap minimum fixed at $y_0 = 0$. In order to put the soliton in motion, we shift the trap minimum from $y_0 = 0$ to a nonzero value at $t = 0$ along the y axis and compute the resulting dynamics from numerical time integration of the GPE system.

In Fig. 7, we show the dynamics of the COM of the two BEC components for different values of the initial shift y_0 in

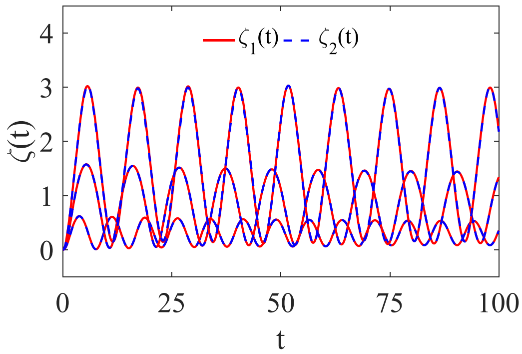

FIG. 8. Same as in Fig. 7, but for $V_2 = -0.5$ and initial displacements $y_0 = 0.2\pi,\ 0.35\pi,\ 0.5\pi$.

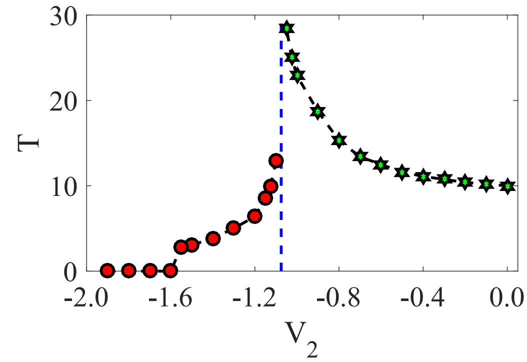

FIG. 10. Period T of the binary soliton vs V_2 for $0 < |V_2| < |V_{2cr}|$ (green stars) and for $|V_2| > |V_{2cr}|$ (red circles). Parameters are fixed as in Fig. 9 for which $V_{2cr} \approx -1.075$.

the absence of the NOL (i.e., with only the LOL acting in the x direction). We see that in this case the motion of the two components is perfectly harmonic with the oscillation period independent of the amplitude. In the presence of the NOL, however, the situation drastically changes.

As it is seen from Fig. 8, when the strength of the NOL is small, the binary BEC executes oscillations around the minimum of the harmonic trap, as expected, but the frequency of the oscillation depends on the amplitude, i.e., the presence of the NOL introduces anharmonicity. By increasing the strength of the NOL while keeping all other parameters fixed, a critical value of V_2 appears (i.e., $V_{2cr} \approx -1.075$ in Fig. 9) above which the self-trapping phenomenon occurs. From Fig. 9 we see that just before the self-trapping transition, the dynamics strongly deviates from harmonic motion, with the trajectory of the center of mass of the binary soliton acquiring zigzaglike profiles.

Note that the oscillations below and above the critical point have different natures; the first occurs around the minimum of the parabolic trap (fixed to $\pi/2$ in the figure) and the second occurs around the minimum of the effective NOL potential at the self-trapping position. In both cases, however, the two components oscillate together on a long timescale with their centers of mass practically overlapped. As the strength of the NOL is further increased beyond the transition point, the soliton becomes dynamically self-trapped inside the NOL effective potential. In Fig. 10, we show the dependence on V_2 of the period, T, of the binary soliton when the oscillation occurs inside the parabolic trap and inside the effective NOL potential, i.e., for $0 < |V_2| < |V_{2cr}|$ and for $|V_2| > |V_{2cr}|$, respectively. The above dynamical behaviors can be qualitatively understood in terms of the NOL potential barrier discussed in the previous section. When the NOL strength is small compared to the critical value, the soliton motion can easily overcome the barrier and the resulting oscillation is harmonic but with smaller

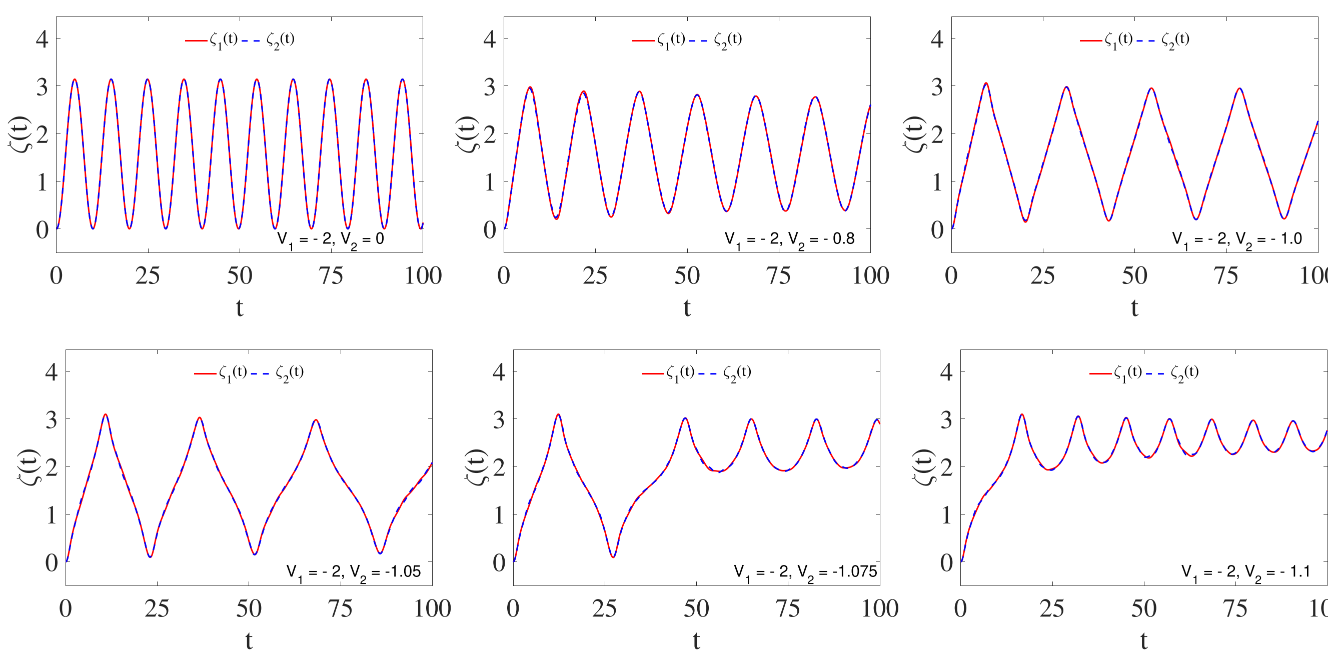

FIG. 9. The center-of-mass coordinate of the first (red solid) and the second (blue dashed) components of binary BEC in a parabolic trap $\beta(y - y_0)^2$ for different V_1, V_2 values, indicated in the panels. Other parameters are fixed as $\gamma_{12} = -2$, $\gamma_1 = -2.0$, $\gamma_2 = 0$, $\mathcal{N}_1 = 3.5$, $\mathcal{N}_2 = 2.5$, $\beta = 0.1$, $y_0 = 0.5\pi$.

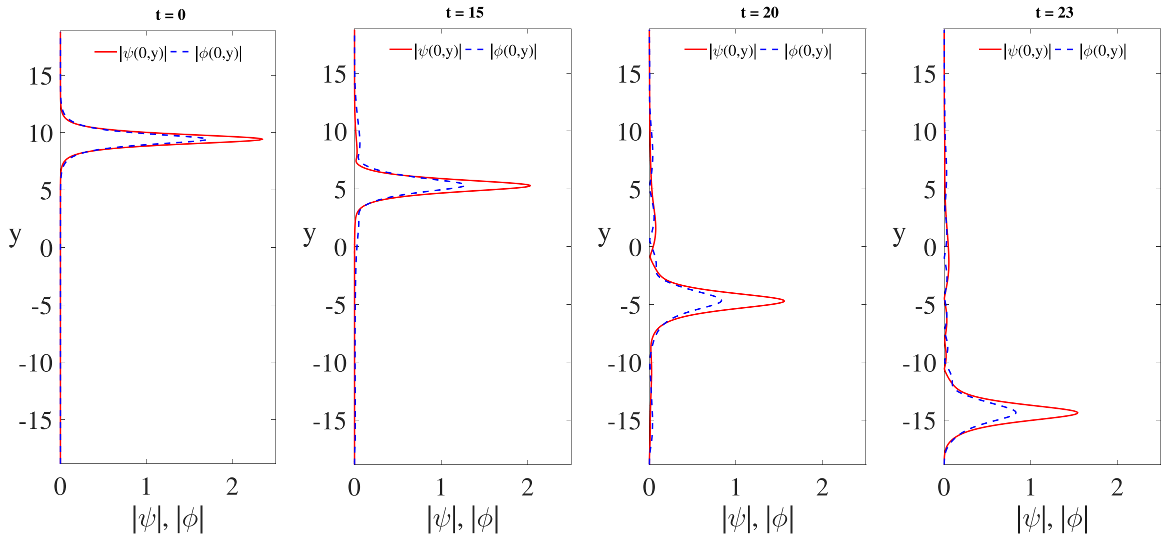

FIG. 11. Density sections at $x = 0$ of the two components $|\psi(0, y)|$ (solid red lines) and $|\phi(0, y)|$ (dashed blue lines) at different instant of times, $t = 0, 15, 20, 23$, starting from the left, respectively. The parameter $\alpha = 0.155$ is just slightly above the critical value $\alpha_{cr} = 0.15$. Other parameters are fixed as $\gamma_{12} = -2.0$, $\gamma_1 = -2.0$, $\gamma_2 = 0$, $V_1 = -2.0$, $V_2 = -1$, $\mathcal{N}_1 = 3.5$, $\mathcal{N}_2 = 2.5$.

frequency with respect to the case $V_2 = 0$. The larger oscillation period observed for $|V_2| \leqslant |V_{2cr}| \geqslant 0$ can be ascribed to the slowing down of the soliton during the overcoming of the barrier. This slowing-down effect increases as V_2 approaches the critical value at which the binary soliton becomes self-trapped. The oscillations in the self-trapped regime $|V_2| > |V_{2cr}|$ obviously depend on the NOL effective potential at the position where the self-trapping occurs. As V_2 is increased above the critical value, the amplitudes and periods of these oscillations decrease, as expected for states localized in strong trapping potentials. For very large NOL amplitudes, the binary soliton becomes fully at rest at a position that in the absence of the NOL, would be of nonequilibrium for a parabolic trap.

B. Linear ramp potential

In this section, we consider a linear ramp potential of the form $\alpha\,(y - y_0)$, with α, y_0 real parameters, mimicking a gravitational field acting on both components in the y direction. The initial conditions are taken as stationary solutions of the $\alpha = 0$ case located at the position $x_0 = 0$, $y_0 = 3\pi$. The linear ramp potential is switched on at $t = 0$, and the time evolution is obtained from direct numerical integrations of the GPE. Numerical results are displayed in Figs. 11–14.

From Fig. 11, we see that for sufficiently small values of the strength of the NOL and for $V_2 = 0$ (not shown for brevity), the binary matter wave is accelerated just as expected for solitons falling in a gravitational field, with only some small deformations of the profiles and some tiny emission of radiation due to the sudden acceleration and switching-on of the potential. By increasing the strength of the NOL and keeping all other parameter fixed, however, we find that there exists a critical value of V_2 above which the binary soliton instead of falling under the action of the gravity remains suspended,

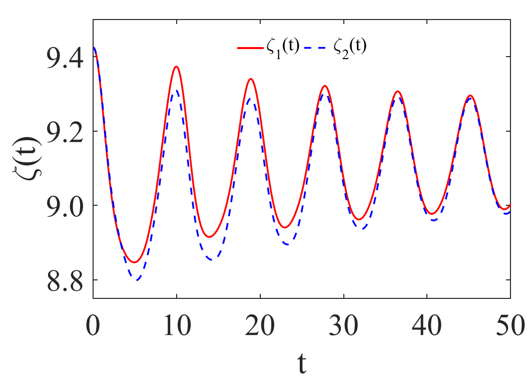

FIG. 12. Time evolution of the COM coordinates of the first (red solid) and the second (blue dashed) components of a binary BEC in the linear ramp potential $\alpha(y - y_0)$ with $\alpha = \alpha_{cr} = 0.15$. Other parameters are fixed as $\gamma_{12} = -2.0$, $\gamma_1 = -2.0$, $\gamma_2 = 0$, $V_1 = -2.0$, $V_2 = -1$, $\mathcal{N}_1 = 3.5$, $\mathcal{N}_2 = 2.5$, $y_0 = 3\pi$. Notice that this parameter setting is the same as for the point $\alpha_{cr} = 0.15$ in Fig. 14.

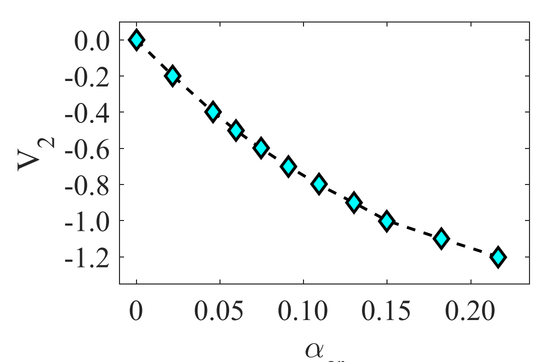

FIG. 13. Critical curve in the parameter plane V_2, α separating the falling regime (region above the curve) from the dynamical self-trapping regime (region below the curve). Other parameters are fixed as $\gamma_1 = -2.0$, $\gamma_2 = 0$, $\gamma_{12} = -2$, $V_1 = -2.0$, $\mathcal{N}_1 = 3.5$, $\mathcal{N}_2 = 2.5$. The dependence of α_{cr} to the intercomponent interaction coefficient γ_{12}. For numerical purposes, we fixed values of different parameters at $\gamma_1 = -2.0$, $\gamma_2 = 0$, $V_1 = -2.0$, $V_2 = -1$, $\mathcal{N}_1 = 3.5$, $\mathcal{N}_2 = 2.5$.

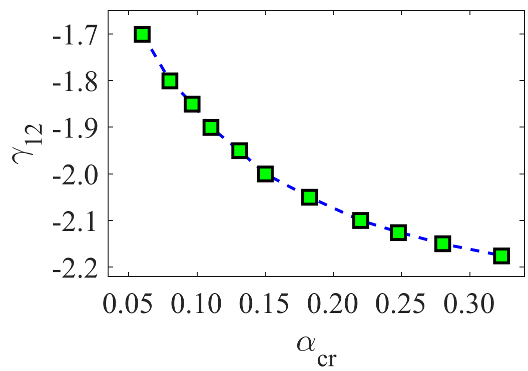

FIG. 14. Critical curve in the parameter plane γ_{12}, α separating the falling regime (region above the curve) from the dynamical self-trapping regime (region below the curve). Other parameters are fixed as $\gamma_1 = -2.0$, $\gamma_2 = 0$, $V_1 = -2.0$, $V_2 = -1.0$, $\mathcal{N}_1 = 3.5$, $\mathcal{N}_2 = 2.5$.

executing oscillations around a fixed position. This is the same DSTP discussed before for the parabolic case.

The critical thresholds for the falling or the DSTP of the binary soliton depend on all system parameters and particularly on the slope of the ramp, the strength of the NOL, and the intercomponent interaction. In Figs. 13 and 14, we show curves in the parameter planes (V_2, α) and (γ_{12}, α) that separate the falling regime (region above the curves) from the dynamical self-trapping regime (region below the curves), for a specific set of the rest of the parameters, respectively.

From these figures, we see that a stronger gravitational field (larger slope of the ramp) requires a stronger NOL amplitude V_2 or a larger intercomponent interaction γ_{12} for the dynamical self- trapping phenomenon to occur. These behaviors can be easily understood in terms of the dynamical self-trapping barrier. Indeed, an increase of the ramp's slope implies a large energy acquired by the soliton, which, in turn, requires a larger potential barrier to stop it.

From Eq. (21), it is clear that the effective NOL potential can be increased either by increasing $|V_2|$ (this explains the curve in Fig. 13) or by increasing the density of the soliton, which can be achieved by increasing the attractive intercomponent interaction so that the binary soliton becomes more focused (this explains the curve in Fig. 14).

In closing this section, we remark that in principle, one could apply the external potentials in the x direction instead of the y direction. We discard this possibility, however, for the following two reasons. First, in this setting, there would be no dynamics in the y direction and therefore no DSTP would occur. Second, in the ramp potential case, the combined action with the LOL would lead, in analogy to what happens in the 1D single-component case (see Ref. [19]), to dynamical instabilities that would destroy the binary soliton.

VI. DISCUSSION AND CONCLUSIONS

Before closing this paper, we feel compelled to discuss advantages of 2D cross-combined LOL and NOL settings and possible practical implications of our results. In general, for the development of soliton applications, the following is important: (i) their stability and (ii) their management, i.e., the possibility to manipulate their motion.

In a multidimensional setting, the first point is already nontrivial due to the presence of collapse, delocalization, etc. It is possible to avoid these adverse phenomena, at least in a region of nonzero measure in the parameter space, by exposing the condensate to the action of a 1D LOL (a 2D LOL would also stabilize the solitons against collapse, but it would limit their mobility). This is true both for the single-component case, as demonstrated in Ref. [17], and for binary solitons, as one can see from the $V_2 = 0$ cases of Figs. 5 and 8. The presence of a NOL in the y direction, although not strictly necessary for existence and stability, allows one to satisfy requirement (ii). Indeed, the control of the DSTP can be used as a tool for moving or stopping solitons in given positions, as shown in the examples discussed above. It is remarkable that in our setting, the management can be done without any physical modification of the system, simply by acting on the external laser fields that control the interactions via the usual (two-body) or the optically induced (NOL) Feshbach resonances. The management of the soliton motion is certainly a fundamental step for experimental and applicative developments.

In conclusion, we have demonstrated, both by variational analysis and by direct numerical integration of the GPE coupled equations, the existence and stability of 2D binary BEC mixtures trapped in a cross-combined lattice consisting of a one-dimensional linear optical lattice in the x direction, for the first component, and a 1D nonlinear OL in the y direction for the second component. Dynamical properties of such binary 2D soliton have been investigated both by phase imprinting and by applying additional external potentials along the constraint direction of the cross-combined OLs. In particular, we have shown the occurrence of the DSTP that allows one to hold a soliton at rest in a nonequilibrium position of a parabolic potential or to prevent a soliton from falling under the action of gravity. The existence of thresholds in the parameter space for the occurrence of these phenomena has also been demonstrated.

ACKNOWLEDGMENTS

The authors would like to thank Dr. B. B. Baizakov for discussions and critical reading of the manuscript. K.K.I. acknowledges the Ministry of Innovative Development of the Republic of Uzbekistan for a three-month financial support within the framework of the program "Short-term scientific internship of young scientists in foreign scientific organizations", and the Department of Physics of the University of Salerno for the hospitality.

[1] O. Morsch and M. Oberthaler, Dynamics of Bose-Einstein condensates in optical lattices, Rev. Mod. Phys. **78**, 179 (2006).

[2] M. Ben Dahan, E. Peik, J. Reichel, Y. Castin, and C. Salomon, Bloch oscillations of atoms in an optical potential, Phys. Rev. Lett. **76**, 4508 (1996).

[3] Y. V. Kartashov, B. A. Malomed, and L. Torner, Solitons in nonlinear lattices, Rev. Mod. Phys. **83**, 247 (2011).
[4] G. A. Sekh, M. Salerno, A. Saha, and B. Talukdar, Displaced dynamics of binary mixtures in linear and nonlinear optical lattices, Phys. Rev. A **85**, 023639 (2012).
[5] S. R. Wilkinson, C. F. Bharucha, K. W. Madison, Q. Niu, and M. G. Raizen, Observation of atomic wannier-stark ladders in an accelerating optical potential, Phys. Rev. Lett. **76**, 4512 (1996).
[6] C. J. Pathick and H. E. Smith, *Bose-Einstein Condensation in Dilute Gases*, 2nd ed. (Cambridge University Press, Cambridge, 2008).
[7] J.-R. Li, J. Lee, W. Huang, S. Burchesky, B. Shteynas, F. C. Top, A. O. Jamison, and W. Ketterle, A stripe phase with supersolid properties in spin-orbit-coupled Bose-Einstein condensates, Nature (London) **543**, 91 (2017).
[8] I. Bloch, Ultracold quantum gases in optical lattices, Nat. Phys. **1**, 23 (2005).
[9] V. A. Brazhnyi and V. V. Konotop, Theory of nonlinear matter waves in optical lattices, Mod. Phys. Lett. B **18**, 627 (2004).
[10] F. Abdullaev, A. Abdumalikov, and R. Galimzyanov, Gap solitons in Bose-Einstein condensates in linear and nonlinear optical lattices, Phys. Lett. A **367**, 149 (2007).
[11] Y. Zhang, Y. Xu, and T. Busch, Gap solitons in spin-orbit-coupled Bose-Einstein condensates in optical lattices, Phys. Rev. A **91**, 043629 (2015).
[12] X. Chai, D. Lao, K. Fujimoto, and C. Raman, Magnetic soliton: From two to three components with SO(3) symmetry, Phys. Rev. Res. **3**, L012003 (2021).
[13] B. B. Baizakov and M. Salerno, Delocalizing transition of multidimensional solitons in Bose-Einstein condensates, Phys. Rev. A **69**, 013602 (2004).
[14] C.-M. Schmied and P. G. Kevrekidis, Dark-antidark spinor solitons in spin-1 Bose gases, Phys. Rev. A **102**, 053323 (2020).
[15] G. C. Katsimiga, S. I. Mistakidis, K. Mukherjee, P. G. Kevrekidis, and P. Schmelcher, Stability and dynamics across magnetic phases of vortex-bright type excitations in spinor Bose-Einstein condensates, Phys. Rev. A **107**, 013313 (2023).
[16] Y. Li, X. Zhang, R. Zhong, Z. Luo, B. Liu, C. Huang, W. Pang, and B. A. Malomed, Two-dimensional composite solitons in Bose-Einstein condensates with spatially confined spin-orbit coupling, Commun. Nonlinear Sci. Numer. Simulat. **73**, 481 (2019).
[17] B. B. Baizakov, B. A. Malomed, and M. Salerno, Multidimensional solitons in periodic potentials, Europhys. Lett. **63**, 642 (2003).
[18] B. B. Baizakov, B. A. Malomed, and M. Salerno, Multidimensional solitons in a low-dimensional periodic potential, Phys. Rev. A **70**, 053613 (2004).
[19] M. Salerno, V. V. Konotop, and Yu. V. Bludov, Long-living bloch oscillations of matter waves in periodic potentials, Phys. Rev. Lett. **101**, 030405 (2008).
[20] H. L. F. da Luz, F. Kh. Abdullaev, A. Gammal, M. Salerno, and L. Tomio, Matter-wave two-dimensional solitons in crossed linear and nonlinear optical lattices, Phys. Rev. A **82**, 043618 (2010).
[21] F. Kh. Abdullaev, A. Gammal, H. L. F. da Luz, and L. Tomio, Dissipative dynamics of matter wave soliton in nonlinear optical lattice, Phys. Rev. A **76**, 043611 (2007).
[22] Y. V. Kartashov, B. A. Malomed, V. A. Vysloukh, and L. Torner, Two-dimensional solitons in nonlinear lattices, Opt. Lett. **34**, 770 (2009).
[23] O. V. Borovkova, Y. V. Kartashov, and L. Torner, Stabilization of two-dimensional solitons in cubic-saturable nonlinear lattices, Phys. Rev. A **81**, 063806 (2010).
[24] Z. Hadzibabic, P. KrAuger, M. Cheneau, S. P. Rath, and J. Dalibard, The trapped two-dimensional Bose gas: From Bose-Einstein condensation to Berezinskii-Kosterlitz-Thouless physics, New J. Phys. **10**, 045006 (2008).
[25] N. L. Smith, W. H. Heathcote, G. Hechenblaikner, E. Nugent, and C. J. Foot, Quasi-2D confinement of a BEC in a combined optical and magnetic potential, J. Phys. B: At. Mol. Opt. Phys. **38**, 223 (2005).
[26] S. Burger, F. S. Cataliotti, C. Fort, P. Maddaloni, F. Minardi, and M. Inguscio, Quasi-2D Bose-Einstein condensation in an optical lattice, Europhys. Lett. **57**, 1 (2002).
[27] X. Ma, R. Driben, B. A. Malomed, T. Meier, and S. Schumacher, Two-dimensional symbiotic solitons and vortices in binary condensates with attractive cross-species interaction, Sci. Rep. **6**, 34847 (2017).
[28] O. V. Borovkova, B. A. Malomed, and Y. V. Kartashov, Two-dimensional vector solitons stabilized by a linear or nonlinear lattice acting in one component, Europhys. Lett. **92**, 64001 (2010).
[29] A. A. Kolokolov, Stability of the dominant mode of the nonlinear wave equation in a cubic medium, J. Appl. Mech. Tech. Phys. **14**, 426 (1975).
[30] Y. S. Kivshar and D. K. Campbell, Peirls-Nabarro potential barrier for highly localized nonlinear modes, Phys. Rev. E **48**, 3077 (1993).
[31] D. Anderson, Variational approach to nonlinear pulse propagation in optical fibers, Phys. Rev. A **27**, 3135 (1983).
[32] We find that in the case $V_2 = 0$, the two trial functions (sech-sech and Gaussian) lead to similar variational results, but the comparison with the exact numerical results in the top panels of Fig. 3 is better for the Gaussian *Ansatz*.
[33] N. G. Vakhitov and A. A. Kolokolov, Stationary solutions of the wave equation in the medium with nonlinearity saturation, RadioPhys. Quantum Electron. **16**, 783 (1973);
[34] For non-cross-combined lattices, e.g., a 2D LOL or a 2D NOL, the two minimizations would be compatible.
[35] W. Bao, D. Jaksch, and P. A. Markowich, Numerical solution of the Gross-Pitaevskii equation for Bose-Einstein condensation, J. Comput. Phys. **187**, 318 (2003).
[36] R. H. Hardin and F. D. Tappert, Application of the split-step Fourier method to the numerical solution of nonlinear and variable coefficient wave equations, SIAM Review Chronicle **15**, 423 (1973).
[37] S.-T. Ji, and X.-S. Liu, Generating ring dark solitons in two-component Bose-Einstein condensates, Phys. Lett. A **378**, 524 (2014).
[38] G. A. Sekh, F. V. Pepe, P. Facchi, S. Pascazio, and M. Salerno, Split and overlapped binary solitons in optical lattices, Phys. Rev. A **92**, 013639 (2015).
[39] The phenomenon of dynamic self-trapping also exists in 1D environments for ordinary (i.e., single-component) BEC solitons. This was apparently unnoticed in previous studies.